The Light and the Dark of Early and Intermediate AMD: Cone- and Rod-Mediated Changes Are Linked to Fundus Photograph and FAF Abnormalities

Elena Rodrigo-Diaz,[1] Humza J. Tahir,[1] Jeremiah M. Kelly,[1] Neil R. A. Parry,[1,2] Tariq Aslam,[1,2] and Ian J. Murray[1]

[1]Vision Science Lab, Faculty of Biology, Medicine and Health, University of Manchester, Manchester, United Kingdom
[2]Vision Science Centre, Manchester Royal Eye Hospital, Manchester University NHS Foundation Trust, Manchester Academic Health Science Centre, Manchester, United Kingdom

Correspondence: Ian J. Murray, Vision Sciences Lab, Room 4.007, Carys Bannister Building, Dover Street, Manchester M13 9PL, UK; ian.j.murray@manchester.ac.uk.

Submitted: August 4, 2019
Accepted: October 24, 2019

Citation: Rodrigo-Diaz E, Tahir HJ, Kelly JM, Parry NRA, Aslam T, Murray IJ. The light and the dark of early and intermediate AMD: cone- and rod-mediated changes are linked to fundus photograph and FAF abnormalities. *Invest Ophthalmol Vis Sci*. 2019;60:5070–5079. https://doi.org/10.1167/iovs.19-27971

Purpose. The purpose of this paper is to describe the extent to which scotopic and photopic measures of visual function predict color fundus photograph (CFP) and fundus autofluorescence (FAF) changes in early and intermediate nonexudative AMD.

Methods. Sixty-nine observers were recruited: 56 AMD patients (mean age, 73 ± 12.98 years) and 13 controls (mean age, 67.77 ± 9.72 years). A nonmydriatic retinal camera was used to obtain stereo fundus photographs and FAF images were recorded with a cSLO Heidelberg Spectralis HRA+OCT. Visual acuity (VA) was measured using an Early Treatment of Diabetic Retinopathy Study chart. Contrast sensitivity (CS) was assessed with a Pelli-Robson chart. Dark adaptation (DA) curves were recorded at 3° eccentricity using a PC-based technique. Analysis of these curves yielded five parameters: cone threshold (CT), cone time constant (CC), cone-rod break (α), slope of the second rod component (S2), and rod-rod break (β).

Results. Both cone and rod sensitivity recovery were grossly abnormal in the patients. The rod recovery slope (S2) most accurately predicted the fundus photograph–based grade and the FAF classification ($\rho = 0.61$ and $\rho = 0.60$, respectively; both $P < 0.0001$). CS showed a strong association with FAF ($\rho = 0.50$, $P < 0.0001$) and with fundus photograph–based grade ($\rho = 0.38$, $P < 0.002$). There was no correlation between VA and either imaging method.

Conclusions. Dynamic, rod-based measures most accurately reflect the severity of early AMD. Although less specific to AMD than DA changes, static photopic abnormalities such as CS also correspond with morphologic changes. Assessment of function in early AMD should include dynamic rod- and cone-mediated measurements of sensitivity recovery.

Keywords: AMD, cones, rods, dark adaptation, morphology/fundus photograph

AMD is a major cause of blindness, affecting 30% of those more than 65 years of age in developed countries.[1–3] For demographic reasons, the incidence of the disease is expected to double over the next few decades.[4] Identifying the disease early and slowing the progression are the most likely management routes in the foreseeable future. AMD is a multifactorial disease in which there is a loss of central retinal photoreceptors due either to geographic atrophy (dry AMD) or to a neovascular event (wet AMD). Dry AMD is characterized by the presence of lipoidal bodies called drusen, which may or may not be accompanied by pigmentary changes.[5] Risk factors such as smoking, poor diet, and genetic predisposition have been described,[6–8] and more recently, the interaction between environmental and genetic factors has been reported.[9] However, less is known about the link between functional abnormalities in early AMD and its clinical presentation. In the present work, we investigate this issue by comparing fundus autofluorescence (FAF) and fundus photograph–based AMD grade with photopic and scotopic visual function in early and intermediate AMD and same-age normal observers.

In severe AMD, profound vision loss and its related problems are well documented.[10] However, in the early/intermediate stages of the disease, the visual consequences are more insidious and difficult to identify.[11] Few functional measures are specific to AMD, with the result that diagnosis and staging lack accuracy. Classically, early AMD diagnosis has been based on the grade of fundus photographs,[12] and this classification has been further developed[13] to recommend the terms early, intermediate, and late AMD. Importantly, the latter study took account of the retinal status of both eyes and described the 5-year risk of developing severe, "late" disease associated with each category. Their findings accord well with the Age-Related Eye Disease Study (AREDS) simplified severity scale.[14]

In recent years, other methods capable of documenting structural changes, such as FAF and spectral-domain optical coherence tomography (SD-OCT), have been used to investigate nonexudative AMD.[1,15–17] Some reports describe the functional correlation between these techniques. For example, Acton et al.[1] described the relationship between retinal thickness and visual field defects using SD-OCT. More recently, Ooto et al.[18] used three imaging techniques, fundus photography, FAF, and SD-OCT, to find a correlation between the severity of subretinal drusenoid deposits (previously called reticular pseudodrusen), contrast sensitivity (CS), and macular micro-

perimetry scores. These findings are in agreement with a recent study by Fraser et al.[19]

FAF can also be used to evaluate the RPE during disease and aging. According to Delori et al.,[20] the accumulation of lipofuscin in the retina accounts for most of the FAF signal. Lipofuscin is a byproduct of partially digested photoreceptor outer segments, and this is related to its increased accumulation with age in the normal eye.[21] In the normal retina, autofluorescence distribution is not uniform across the retina, with a gradual decrease in the inner macula to the foveola due to the masking effect of the macular pigment.[22,23] Autofluorescence that is outside normal limits is considered pathologic, whether it is too low or too high. Hyperautofluorescence is associated with the excessive concentration of lipofuscin and is thought to be linked with photoreceptor degeneration. Hypoautofluorescence is likely to be due to degenerative changes of RPE cells.[24,25] Changes in FAF have been studied in early AMD[26] and compared with fundus photographs and SD-OCT.[15,16]

CS has been tested in many clinical trials of AMD.[27–30] There is, however, some controversy regarding its importance. For example, Midena et al.[31] and Feigl et al.[32] found CS to be affected in early AMD compared with age-matched normal subjects, whereas Owsley et al.[30] reported no such effects. Thus, the association between CS and structural changes remains unclear. CS has advantages over visual acuity (VA) in that VA tests only the central foveal cones, whereas CS tests a larger area of retina. CS is, however, abnormal in many ocular conditions and usually represents the function of cones only.

The link between rod function and early AMD has been established for some time.[33,34] The ratio of cones to rods in the macula is approximately 9:1,[35] and it is therefore likely that, by the time patients notice changes in their photopic vision, they will have lost many millions of rods.[34,36–40] Classically, the dynamics of cone and rod function are assessed by exposing the eye to a photobleach and plotting the recovery of sensitivity against time. As has been known for many years,[41–43] this sensitivity recovery function, called the dark adaptation (DA) curve, is composed of cone and rod components. The photobleach depletes the concentration of opsins in the photoreceptors resulting in profound vision loss. Sensitivity recovers in two distinct phases, one mediated by cones and the other by rods.

The DA curve is now accepted as an accurate biophysical assay of the ability of the rods and cones to regenerate their photopigment, as described in detail by Lamb and Pugh.[42] The rate of recovery in the rod-mediated section of the curve is referred to as S2 and has been described as a biomarker for AMD.[44] Abnormal S2 is considered one of the first signs of early disease.[45] In a recent study, Dimitrov et al.[46] showed an association between photopic and scotopic function and a detailed fundus photograph–based AMD grading scheme. The presence of both rod and cone involvement was further confirmed by Luu et al.,[47] who showed a correlation between color microperimetry and color fundus severity scale. Sevilla et al.[48] confirmed the sensitivity of rod dynamics to the disease and showed a link between OCT findings and DA. A clear picture is emerging from the literature that dynamic measures, involving sensitivity recovery from a bleach, are a particularly sensitive index of underlying pathology in dry AMD. There is a sound physiologic basis for this.[49] Such techniques were used in the investigation of dry AMD by Jackson et al.,[50] Murray et al.,[51] and, more recently, Tahir et al.,[40] who confirmed the existence of both photopic and scotopic abnormalities in early AMD.

Both cones and rods are dependent on the RPE–Bruch's membrane complex for delivery of essential nutrients and removal of waste products during sensitivity recovery. It is clear that a detailed understanding of the link between morphologic and functional abnormalities in the context of the efficiency of the RPE–Bruch's membrane complex will be important when unraveling the many factors contributing to the development and management of dry AMD. With this in mind, we set out to investigate specifically the relationship between FAF, fundus photographs, and the efficiency of rod- and cone-mediated photoreceptor function in early AMD.

Methods

Patients

A total of 56 AMD patients and 13 age-matched normal observers were recruited. The AMD group (mean age ± SD, 73 ± 12.98 years) comprised 24 males and 32 females. The control group (mean age, 67.77 ± 9.72 years) comprised 6 males and 7 females. The study was approved by the UK National Health Research Ethics Service, North West Committee. The research followed the tenets of the Declaration of Helsinki.

The AMD patients responded to an advertisement at the Manchester Royal Eye Hospital or were recommended by an ophthalmologist. Some patients were recruited from local ophthalmic practitioners. Controls were recruited from university staff and local advertisements. Informed consent was obtained from all participants after the nature of the investigation was explained. Power was calculated on S2 and color fundus grade. Eligibility criteria were as follows: (1) age ≥ 55 years old; (2) AREDS grade 0 or 1 for subjects in the normal group and AREDS grade 2 or 3 for subjects in the early AMD group according to the AREDS five-step classification system[52]; (3) no other ocular disease such as glaucoma or cataracts in the study eye; and (4) VA 6/12 (logMar 0.3) or better in the study eye. In cases where both eyes had the same AREDS grade, the eye with worse VA was selected as the study eye. There were no cases where there was a clear AMD grade 2 in one eye and AMD grade 3 in the fellow eye.

Fundus Images

Stereo color fundus photographs were obtained with a TRC50DX nonmydriatic retinal camera (Topcon, Tokyo, Japan) with a 30° wide-angle lens, after pupil dilatation (1% tropicamide). For initial recruitment, fundus images of participants were graded by two graders (TA and ERD) according to the AREDS five-step classification system. Nine healthy normal observers were graded as AREDS 0, and 4 were graded as AREDS 1. In the patient group, 24 were graded as AREDS 2 and 32 as AREDS 3. For later comparison with the functional measures, the images were regraded in detail according to the International Classification and Grading System[12] (Table 1).

Fundus Autofluorescence

FAF images were recorded with a cSLO confocal scanning laser ophthalmoscope (Heidelberg Spectralis HRA+OCT; Heidelberg Engineering, Heidelberg, Germany) with a 30° wide-angle lens, using 488-nm excitation (argon laser) and recorded emission above 500 nm (barrier filter). Patients were categorized into one of eight abnormal FAF phenotypic patterns according to the classification of Bindewald et al.,[15] which is illustrated in Table 2. Twenty-two were classified as normal, 19 as minimal changes, 8 as focal increased, 5 as patchy, 5 as lacelike, 5 as reticular, and 4 as speckled patterns. Images were classified independently by two assessors. Note that it was not possible to obtain FAF images from one of the AMD patients; therefore, for FAF, $n = 68$.

Table 1. Distribution of the Study Population ($n = 69$) in Groups Corresponding to a Five-Step Severity Scale Depending on Clinical Signs[12]

Group	Description	n
1 Control (normal)	No presence of drusen or questionable with small size < 63 μm, no pigmentary changes (increased or depigmentation) and no GA	13
2 AMD (small drusen)	Five to 15 small drusen (<63 μm), with no pigmentary changes and no GA	9
3 AMD (pigmentary changes)	Small drusen with pigmentary changes (<63 μm) consistent with AMD and no GA	5
4 AMD (intermediate drusen)	Small or at least one intermediate druse (<125 μm) with or without pigmentary changes and no GA	12
5 AMD (large drusen)	Intermediate or at least one large druse (>125 μm) with or without pigmentary changes and noncentral GA	30

GA, geographic atrophy.

Visual Acuity

VA was measured using an internally illuminated Early Treatment of Diabetic Retinopathy Study (ETDRS) chart at 4 m under photopic conditions (100 cd/m^2). Observers were asked to read all the letters they could recognize with the test eye, starting from the top left letter in the first row. Results were recorded in logMAR units.

Contrast Sensitivity

CS was assessed using a Pelli-Robson chart (Haag-Streit, Harlow, UK) as the number of correctly identified letters. Data were expressed as logarithm of sensitivity (log CS).[53] Luminance of the chart was 100 cd/m^2.

Dark Adaptation

DA was measured psychophysically using a PC-based system as previously described.[39,40,54–57] The test was conducted monocularly in the study eye. The subjects wore their best optical correction for the test distance (90 cm), and the fellow eye was covered using an eye patch. Pupils were dilated using 1% tropicamide (Bausch and Lomb, Rochester, NY, USA) so that pupil diameter ≥5 mm was achieved. Prior to the DA test, a calibrated photographic flash (Speedlight SB800, Nikon, Tokyo, Japan) of 0.9 ms duration was used to bleach between 70% and 99% of the photopigment of the tested retinal area. The integrated intensity of the flash was measured using a PR1500 spotmeter (Photo Research, Burbank, CA, USA) in radiance mode and a CED1401 smart interface (Cambridge Electronic Design Ltd., Cambridge, UK). Depending on the pupil size (mean, 5.3 ± 0.7 mm), the intensity of the flash was between 5.91 and 6.08 log scot.td.s.

The setup is illustrated in Figure 1. The bleach was localized by carefully aligning the flash with the tested retinal area using a semitransparent mirror. A chin and forehead rest was used to maintain the alignment of the participant's eye with the red fixation target. Sensitivity recovery recording started 10 seconds after the exposure to the flash. Thresholds were measured using a modified method of adjustment; the intensity of the stimulus was adjusted from below threshold until it was just detected, and this point was defined as threshold. The intensity was then reduced below threshold and was again slowly increased until it was detected. This procedure continued until enough points were recorded to reach the β-point, also called the rod-rod break. In cases where the β-point was not reached, the maximum testing time was set at 60 minutes.

The stimulus was an arc-shaped segment at 3.0° eccentricity (CIE 1931 chromaticity coordinates: $x = 0.31$, $y = 0.316$). It was presented on a black background using a calibrated and γ-corrected high-resolution CRT monitor (Sony GDM-F500R, Sony, Tokyo, Japan) in the inferior visual field. The small fixation cross was masked with a red filter. The screen was vertically divided in two equal parts to delineate stimulus positions 1 and 2 (Fig. 1).

To ensure near-zero background luminance, the monitor was covered with a black cardboard mask with four apertures corresponding to the stimuli and fixation crosses. Stimuli were generated using a ViSaGe stimulus generator (Cambridge Research Systems, Rochester, UK) and a modified version of the Visual Psychophysics Engine software written by one of the authors (NRAP).

To expand the luminance range of the CRT, neutral density (ND) filters were used.[38] The left half of the monitor was covered with a 1.2 log ND filter and the right half with a 3.6 log ND filter, giving a total luminance range of about 6.5 log units (0.8 to −5.7 log cd/m^2). The stimulus was square-wave modulated at 1 Hz and initially presented at intensity 0.8 log cd/m^2. The stimulus and fixation target firstly appeared at position 1 and automatically shifted to position 2 when the observer sensitivity increased so that the stimulus intensity was reduced below −2.5 log cd/m^2.

DA curves were plotted as log threshold in cd/m^2 versus time in minutes. Individual DA curves were fitted with a nonlinear regression function as described by McGwin et al.[58] and implemented in a custom Matlab script (MATLAB 2013a; The MathWorks, Inc., Natick, MA, USA) as in Patryas et al.[55]

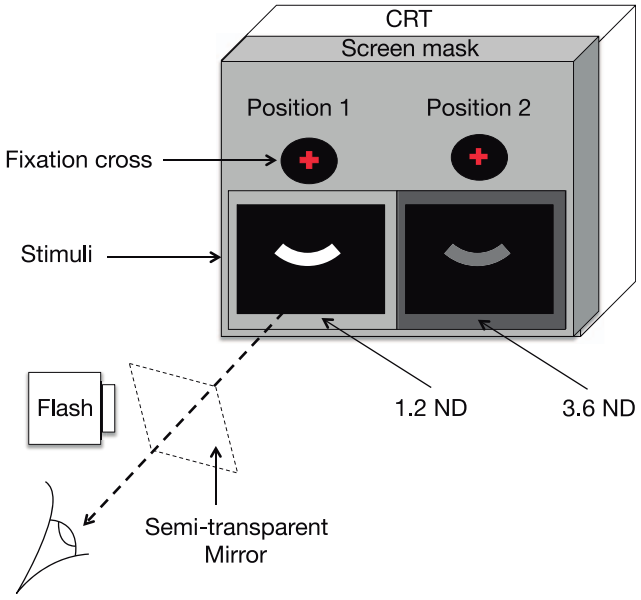

Figure 1. Experimental setup. When the threshold fell below −2.5 log cd/m^2, the fixation cross and the stimulus moved to position 2 where an additional 2.4 ND filter was attached. This gave a total filtered luminance range of 6.5 log units (0.8 to −5.7 log cd/m^2). The location of the photobleach was controlled by aligning the flash with the stimulus (at position 1) through the semitransparent mirror.

Table 2. Distribution of FAF Images in This Study ($n = 68$) According to the Classification of Bindewald et al.[15]

Pattern	Description	n	Category/Groups
Normal	Normal homogeneous background fluorescence with decrease at the foveola due to the effect of the macular pigment	22	Normal
Minimal change	Minimal variation of irregular increase or decrease in FAF background. No obvious topographic pattern.	19	Minimal change
Focal	At least one well-defined spot of substantially increased FAF (>200 μm). May be surrounded by a darker halo.	8	Focal + patchy
Patchy	Multiple large areas (>200 μm) of increased FAF. Less well-defined borders.	5	
Linear	At least one linear area of well-defined increased FA.F	0	
Lacelike	Several branching linear structures of increased FAF. Poorly defined borders. May correspond to hyperpigmentation or to no visible abnormalities in CFP.	5	Other patterns
Reticular	Multiple small areas (<200 μm) of decreased FAF with surrounding increased AF lines. Pattern usually found in a supratemporal location	5	
Speckled	Various FAF abnormalities visible in a larger area of the image.	4	

and Tahir et al.[40,54] As shown in Figure 2, the recovery function is most accurately depicted as being divided into an initial cone-based component followed by two rod-based phases.[41,49] The curve-fitting procedure typically yields seven parameters. In some cases, a simplified version of the modeling was performed for subjects who did not reach the β-point after 60 minutes. In these cases, the β-point was excluded from the original seven-parameter model so that the data were described by a five-parameter model. Data from 64 observers were optimally described with the seven-parameter model and those from five observers were best described with the five-parameter model. Note that in some patients, we did not extract S3 because the maximum time for each DA measurement was set at 60 minutes, and this did not allow sufficient data to capture the S3 slope. In a previous paper,[40] we tested two locations. The data from the inner location (3.0°) are used here because they separate rod and cone function optimally. It also corresponds to pan-retinal activity as obtained from the imaging techniques and can be regarded as a proxy for more global function. Cone coefficient is the parameter that starts the curve fitting algorithm. It is not used in the analysis.

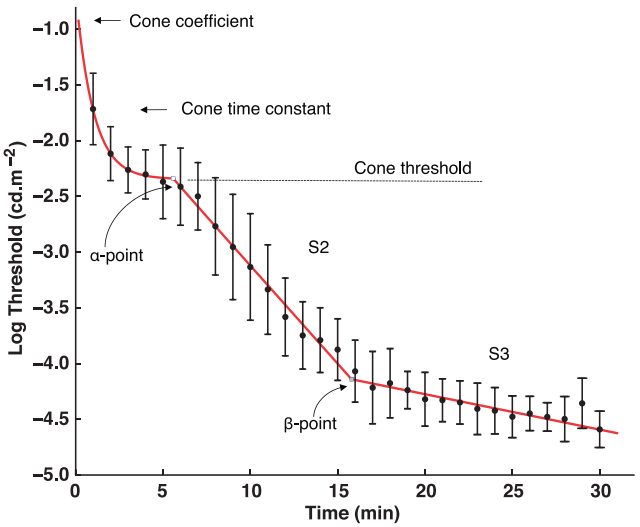

Figure 2. DA curve for normal observers ($n = 13$). The different components of the DA curve are labeled. The data are divided in to 1-minute bin widths for clarity. *Data points* are means and the *error bars* are SDs. The model depicted by the *line* though the data illustrates the cone-mediated component of the curve, the two inflexion points, α and β, and the second and third rod-mediated components, S2 and S3, respectively. Note S3 and cone coefficient are not included in the analysis.

Data Analysis

Patients were categorized into different groups according to the grading of color fundus photographs (Table 1).[12,52] For the comparisons with other modalities, FAF images were divided into four groups from the scheme in Table 2 derived from Bindewald et al.[15] Thirteen eyes had normal macular health and 55 had early AMD. Statistical analysis was performed with IBM SPSS software version 22 (IBM-SPSS, Inc., Chicago, IL, USA). Where the data were not normally distributed (as in the visual tests), differences were analyzed with the Kruskal-Wallis test with further post hoc analysis with Bonferroni correction for pairwise comparisons. The associations among structural and functional changes were tested using Spearman's rank correlation coefficient. Statistical significance was set at 0.05.

Results

Link Between Color Fundus Photograph and FAF Abnormalities

Figure 3 shows the relationship between color fundus changes and the FAF categories. The horizontal axis indicates the fundus photograph–based grading groups (Table 1), whereas the bars illustrate the frequency distribution of FAF categories. White bars represent normal FAF, striped bars represent minimal FAF changes, a starry pattern corresponds to focal or patchy FAF patterns, and black represents the "other" group, which is a combination of lacelike, reticular, and speckled FAF patterns as described in Bindewald et al.[15]

All patients with normal colour fundus photographs had normal FAF. In the group of small drusen, four (50%) presented with normal FAF, three (37.5%) had minimal FAF changes, and one (12%) showed a reticular pattern in the FAF image. The group with pigmentary changes ($n = 5$) in fundus images showed a variety of different FAF patterns without any significant trend; one patient had normal FAF, two had minimal changes, one had a focal pattern, and one a speckle pattern.

In the intermediate drusen group ($n = 12$), 11 (92%) exhibited FAF abnormalities: one had normal FAF, six had minimal changes, two had focal patterns, one had a patchy pattern, one had a lacelike pattern, and one had a reticular pattern. The large drusen group showed most abnormalities in FAF: three were normal, eight had minimal changes, five presented a focal pattern, four had a patchy pattern, four had a lacelike pattern, three had a reticular pattern, and three had

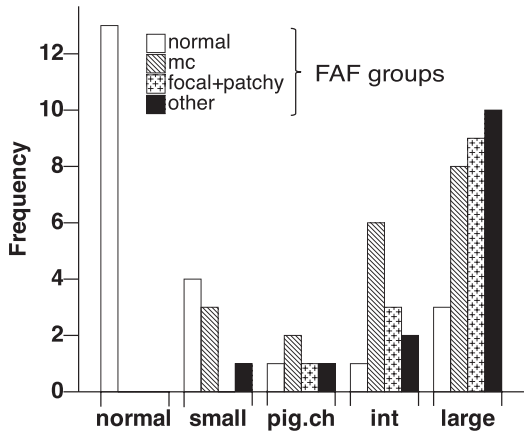

FIGURE 3. Relationship between AMD grade (horizontal axis) and FAF category. FAF groups are shown in the legend. See text describing the other FAF category.

speckled patterns. Note that there were a handful ($n = 3$) of patients with normal FAF but large drusen.

Despite these disparities, there was a strong overall positive association between the two imaging modalities (Spearman's $\rho = 0.625$; $P < 0.001$). This nonparametric technique relies simply on ranking the data and applying the Pearson correlation coefficient. Hence, when more than 90% of patients having intermediate or large drusen show FAF abnormalities and 80% of the patients in the pigmentary changes group showed some FAF abnormality, the analysis inevitably indicates the two methods are associated. The most common FAF pattern in the patient population ($n = 55$) was minimal changes (41.3%), followed by the focal/patchy patterns (28.2%), lacelike patterns (13%), reticular patterns (11%), and speckled patterns (6.5%), suggesting that FAF changes based on the scheme of Bindewald et al.[15] (Table 2) are at least partly linked to severity of AMD.

These observations illustrate that gross AMD fundus abnormalities are invariably reflected in FAF images (see Discussion). The implication is that combining both techniques may have advantages for assessing the clinical significance of drusen and other abnormalities, a point made explicitly in Landa et al.[16] To understand the results of the imaging better, their relationship with the functional tests is explored below.

DA Parameters Compared With Imaging Modalities

Figure 4 shows the relationship between the five main parameters of the DA, the fundus photograph–based AMD grade, and FAF classifications. The eight categories in Table 2 have been collapsed to four, based on the association between early AMD and FAF described by Bindewald et al.[15] Hence, we created a category termed focal and patchy, which combines categories 3 and 4 from Table 2, and an other category, which includes the remaining patterns.

The DA parameters that can be attributed purely to rod function (S2 and β-point) appear in rows 1 and 3, respectively of Figure 4. Inspecting Figure 4 suggests that they best predict changes in AMD grade and the FAF category, and the analysis confirms this. For the rate of rod recovery (S2) in particular, the association ($\rho = 0.60$, $P < 0.001$) is high, indicating a clear link with the morphologic changes in both imaging techniques (note the negative units in the *y*-axis for S2 in the first row). This means better performance (faster recovery) is indicated by larger negative values. There were statistically significant effects in S2 in patients having intermediate ($P = 0.018$) or large drusen ($P < 0.001$) compared with healthy normal subjects, indicated by asterisks in Figure 4. In the autofluorescence images, statistically significant differences are evident in patients with focal or patchy FAF patterns ($P = 0.022$) and the other FAF category ($P < 0.001$) compared with normal subjects.

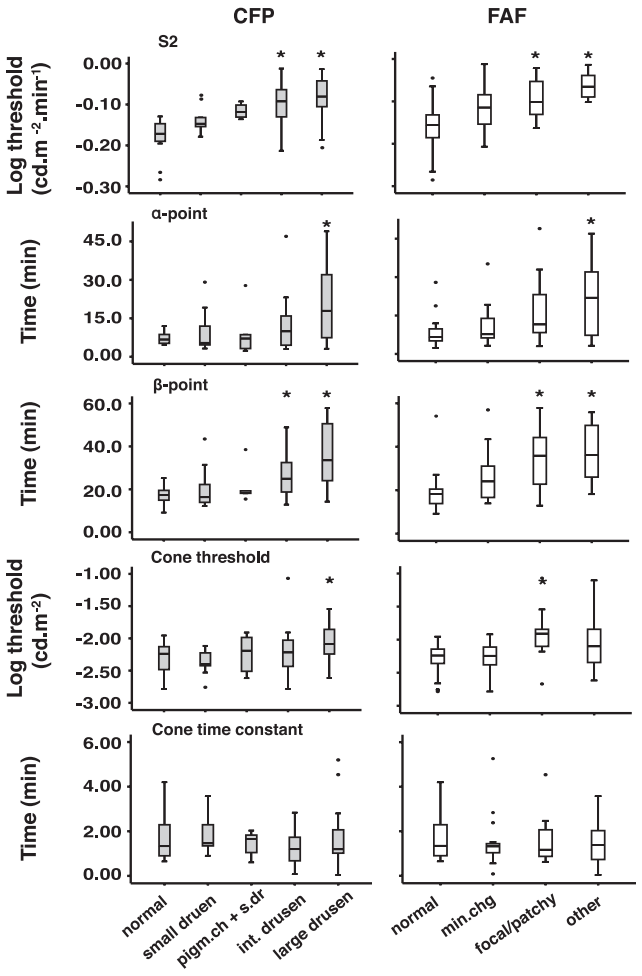

FIGURE 4. Relationship between DA parameters (*rows*) and morphologic changes reflected in fundus photograph grade (*left column*) and FAF (*right column*). Significant differences (after Bonferroni correction) compared with healthy normal subjects are indicated by an *asterisk*. *x*-axes represent the different groups according to the scaling of the images based on Tables 1 and 2. *y*-axes indicate the DA parameters. In each *box*, the *central line* is the median, and the *edges of the box* are the interquartile range. *Whiskers* indicate most extreme data points, and outliers are plotted individually as *circles*.

Row 2 in Figure 4 illustrates the link between rod-cone break (α-point), essentially a photopic measure, and the morphologic changes. Here, the data suggest a slightly reduced association between structural and functional changes compared with S2.

The Kruskal-Wallis test by ranks was used to analyse the data because some parameters were normally distributed (according to the Kolmogorov-Smirnoff test) and others were not. The data are presented in Table 3. As an omnibus procedure, Kruskal-Wallis tests the hypothesis that there are significant differences between the categories of morphologic changes revealed by the imaging, according to the dependent variables derived from the various measures of function.

The *H* statistic suggests that FAF grading has a weak but significant effect on VA. However, in the post hoc analysis after

Table 3. Kruskal-Wallis Analysis General Results for CFP and FAF

	DA Parameters						
Image Modality	**S2**	**α**	**β**	**CT**	**CC**	**VA**	**CS**
CFP							
H (4)	24.32	12.58	24.20	11.70	2.15	3.43	12.84
P	**<0.001**	**0.014**	**<0.001**	**0.020**	0.71	0.49	**0.012**
FAF							
H (3)	24.02	7.90	18.60	13.86	0.53	8.65	16.33
P	**<0.001**	**0.048**	**<0.001**	**0.003**	0.91	**0.034**	**0.001**

Significant differences between patients and normal subjects are indicated in bold. H, Kruskal-Wallis test statistic (degrees of freedom in brackets).

applying Bonferroni correction to the pairwise analysis, this effect was not sufficiently strong to reach statistical significance.

Correlation coefficients are presented in Table 4. There were strong associations between the fundus photograph, AMD grade, and all DA parameters apart from cone time constant (CC). Of all DA parameters, S2 best predicted fundus grading ($\rho = 0.61$, $P < 0.0001$). Similarly, S2 showed the strongest association with the severity of FAF changes ($\rho = 0.60$, $P < 0.0001$). It is clear that other DA parameters, notably the rod-rod break (β-point), also predicted the FAF grading ($\rho = 0.55$, $P < 0.001$).

Photopic Visual Function Compared With Imaging Modalities

Regarding the photopic DA parameters (i.e., those mediated by cones [cone-rod break, cone threshold, and cone time constant]), the highest association was between cone-rod break (α) and fundus photograph grade ($\rho = 0.41$, $P < 0.001$). Cone-rod break and FAF categories showed correlation ($\rho = 0.34$, $P = 0.005$). Correspondingly, there were significant differences in α between normal subjects and patients in the large drusen group, and this applies to both FAF ($P = 0.048$) and color fundus photograph (CFP) ($P = 0.014$). Cone threshold also exhibited a moderate correlation with CFP and FAF ($\rho = 0.36$ and 0.35; $P < 0.001$ and 0.004, respectively), whereas cone time constant did not appear to have a relationship either with CFP or FAF. It is important to recognise that α can be regarded as a separate predictor of dysfunction from S2 as discussed in Tahir et al.[40]

Contrast Sensitivity

CS and VA are static measures of photopic function. Their links with the morphologic changes are illustrated in Figure 5. The correlation was higher with the FAF ($\rho = 0.50$, $P < 0.001$) images than with fundus photograph grade ($\rho = 0.38$, $P < 0.002$). CS clearly decreases progressively, with the FAF scale showing significant differences for all the patients presenting any abnormal FAF apart from minimal changes ($P = 0.004$ for focal/patchy pattern and $P = 0.001$ for other patterns). Compared with the fundus grade, there is a slight decline in CS, but significant differences were found only in the large drusen group ($P = 0.008$).

Visual Acuity

There was no correlation between VA and fundus photograph–based grade. There was, however, a mild link between VA and FAF ($\rho = 0.28$, $P = 0.02$).

Discussion

The relationship between structural and functional changes in early and intermediate AMD was explored by obtaining scotopic and photopic measurements from a group of 56 patients and 13 controls. Participants were categorized from color fundus photographs and FAF images. The main aim of the study was to identify those aspects of structural change that best predict photopic and scotopic visual dysfunction. A secondary aim was to describe the correspondence between the two imaging techniques.

We confirm that rod sensitivity recovery appears to be the first casualty in early AMD but, as emphasised in Tahir et al.,[40] careful analysis of the DA curve also reveals abnormalities in cone dynamics. The steepness of the rod-mediated portion of the dark adaptation curve, S2, most closely reflects disease severity in terms of fundus grade and FAF. Although the FAF classification is largely descriptive, the different categories adopted are faithfully reflected in the S2 data. As far as we are aware, this is the first study to provide a systematic analysis of FAF data and scotopic and photopic visual function in AMD. It is clear that better understanding of the different stages of early-stage disease will be achieved by linking dynamic measures derived from DA with other biomarkers, as discussed in Dimitrov et al.[45] Note, however, that CS, a static measure of

Table 4. Correlation Coefficients Between the Structural Features in Fundus Images and Functional Visual Tests

	DA Parameters						
Image Modality	**S2**	**α**	**β**	**CT**	**CC**	**VA**	**CS**
CFP							
ρ	0.61	0.41	0.61	0.36	0.02	0.15	−0.38
P	**<0.001**	**<0.001**	**<0.001**	**<0.001**	0.78	0.21	**0.002**
FAF							
ρ	0.60	0.34	0.55	0.35	0.04	0.28	−0.50
P	**<0.001**	**0.005**	**<0.001**	**0.004**	0.72	**0.02**	**<0.001**

Significant differences between patients and normal subjects are indicated in bold. *P* values are Bonferroni corrected.

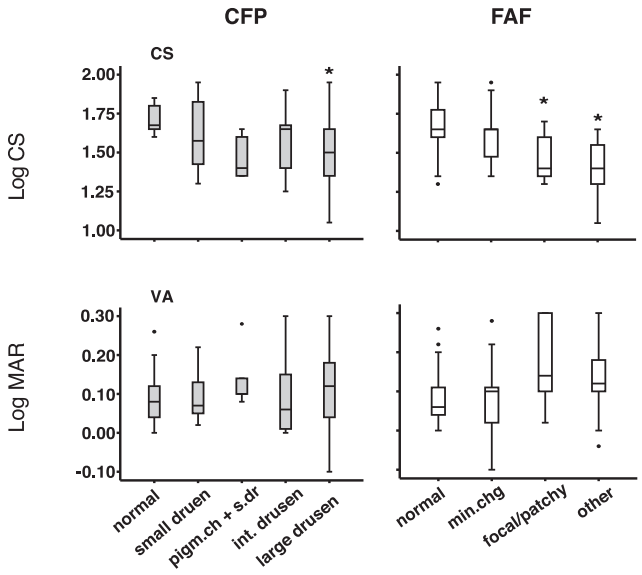

FIGURE 5. Relationship between CS and VA and morphologic changes observed in fundus grade (*left column*) and FAF (*right column*). Significant differences compared with normal healthy observers are indicated by an *asterisk*. In each *box*, the *central line* is the median, and the *edges of the box* are the interquartile range. *Whiskers* indicate most extreme data points, and outliers are plotted individually as *circles*.

photopic vision, is also a reasonably good predictor of FAF changes but not of the fundus photograph grade.

It is important to recognize the theoretical basis on which the DA curve is founded. The time course of recovery is an accurate assay of opsin regeneration in photoreceptor outer segments as described by Lamb and Pugh.[42] As such, it reveals the rate of recovery of rhodopsin, which in turn depends on the diffusion characteristics of the RPE–Bruch's membrane complex. The technique is therefore readily justified clinically because its intimate link with the underlying physiology means it is likely to be an accurate indicator of the effectivity of new therapies. This applies especially as there are now techniques for speeding up the data collection and analysis process.

Comparison of Imaging Modalities

We found an overall strong correlation between fundus photograph grade and the FAF classification ($\rho = 0.625$, $P < 0.001$; Fig. 3). It is important to point out, however, that the statistics hide some substantial disparities between the data from the two methods. In describing their categorization scheme, Bindewald et al.[15] noted that areas with either increased or decreased FAF signal may or may not correspond to clinically significant drusen and pigmentary changes. Although they are closely associated, it is obvious from these data that the FAF images represent a different manifestation of underlying pathology from fundus photographs. As the disease progresses, it is more likely that abnormalities in both methods will be encountered. As our data show, the categorizations in Table 2 represent disease progression, but the geographical distribution of abnormalities is frequently different to that seen in color fundus photographs.

In their study, Landa et al.[16] used SD-OCT to compare the ultra-structure of drusen and FAF images. They reported a close correlation between the two methods for larger, but not small, drusen. Relevant to the present study, they also found that FAF predicted the disruption of the junction between inner and outer photoreceptor segments according to the SD-OCT images. As might be expected, this structure is thought to be closely linked to receptor function, and there is evidence for this.[59] Note that small isolated hard drusen are not considered a sign of AMD and these are frequently not reflected in FAF. However, Dimitrov et al.[46] reported DA abnormalities in 59 patients with small hard drusen compared with patients with no drusen, and this effect reached statistical significance, at least for pure rod-mediated regions of the DA curve. They speculated that slowed rod recovery is likely to be the precursor of future pathology and may therefore provide further insight into the natural history of the early stages of the disease.

Significance of S2, α, and β

As illustrated in Figure 2, sensitivity to recovery after a bleach is composed of three separate components. Initially, there is a rapid initial cone-mediated region that culminates in the inflexion point between cone and rod function called the α-point. This is followed by S2, which is a direct representation of rhodopsin regeneration.[41,42,49] Finally, S3 follows the β-point. This is kinetically distinct from S2 in that it has a longer time constant.[42] The cone-mediated region of the DA curve is almost certainly faster because cone opsins use an intraretinal pathway, probably based in the Müller cells, to regenerate after exposure to a bleach. As discussed in Tahir et al.,[40] this would explain the lack of correlation between α and S2 in early and intermediate AMD, suggesting that α is a unique predictor of underlying pathology. The point in disease progression when cones are first affected may be prognostically important. It is well known that large numbers of early-stage patients have slowed DA, and these are invariably accompanied by drusen. The involvement of cones may represent a tipping point from early, relatively benign, AMD toward more severe sight-threatening stages of the disease.

We have not measured the slope of S3 for the reasons described previously. Instead, we measured β, which represents the transition time between S2 and S3. S3 is mediated purely by rods and is described as being linked to the "absolute dark light" of the fully dark-adapted retina. The dark light (intrinsic photoreceptor noise, for example) will add to component S3, resulting in a "round out" as sensitivity tends toward maximum. As a result, it has a shallower slope (approximately 0.6 LU/min in normal subjects) and has a different dependence on S2 as a function of bleach intensity. This component is discussed in detail in Lamb and Pugh.[42]

It is well known that S2 is systematically reduced in the normal older eye, whereas the cone-mediated DA parameters are not.[37,55,60] The slowing of specifically rod-mediated DA is likely to be linked to the known age-related changes in Bruch's membrane, namely overall thickening, loss of elasticity, and the formation of a lipid wall. These result in impaired exchange of retinoids and other metabolites between RPE and the photoreceptors.[54,61] In early AMD, these effects are exaggerated by the presence of lipid-rich drusen and basal lamina deposits that accumulate between Bruch's membrane and the RPE. The result is slowed DA, despite normal photopic vision,[46,62] and this is consistent with the observations of patients with early AMD who frequently report night vision problems.[63]

Comments on Other Functional Measures

Our data also indicate that contrast sensitivity appears to be impaired in parallel with fundus photograph grade and FAF abnormalities (Fig. 5). In fact, contrast sensitivity appears, from these data, to be more closely linked with FAF. There is no statistical association with visual acuity. This may be because

the latter reflects the integrity of only the central (1.5°) foveal region of the retina. Contrary to Owsley et al.,[30] we found significant differences in CS between eyes with early AMD and those without. This discrepancy is probably due to differences in data analysis. They compared normal against early AMD, whereas we divided the early AMD participants into four groups, finding significant CS differences only between the large drusen group and normal. Comparably with this study, Kleiner et al.[27] showed a loss of CS with increasing drusen severity.

Other measures of association between structure and function support our data. As discussed earlier, Ooto et al.[18] established the presence of pseudo-drusen as a significant predictor of microperimetry score. Similarly, Fraser et al.[19] found significantly reduced sensitivity and rod dynamic recovery in AMD patients with reticular drusen compared with AMD patients without reticular drusen and with normal subjects. Midena et al.[64] reported reduced macular sensitivity measured by microperimetry in areas with altered FAF. Scholl et al.[65] compared areas of increased or decreased FAF with normal subjects and described a correlation of retinal areas of increased FAF with scotopic sensitivity. It should be noted that structure/function links might be important at different stages of the disease.

These findings support the notion that hyperautofluorescence is associated with excessive concentration of lipofuscin and is linked with photoreceptor degeneration. By contrast, Gliem et al.,[66] using quantitative FAF, found no increased lipofuscin-related FAF in eyes with early-stage AMD. Reduced FAF levels could be explained by decreased lipofuscin accumulation due to reduced photoreceptor density or a slowing of the visual cycle, although direct evidence for this idea is still needed. For this analysis, we used the different patterns of FAF described by Bindewald et al.[15] specifically for early AMD subjects.

Limitations of the Study

FAF imaging has its limitations. Media opacities, especially of the crystalline lens, may impair adequate analysis of the images. Our data do not allow absolute quantitative measurement of the FAF signal, and this may impose minor limitations to their interpretation. Absolute values of the FAF signal allow the identification of abnormal FAF signals over a period of time, and this was not appropriate here. Of course, in future studies, tracking changes over time in both FAF and other imaging modalities such as OCT will be clinically valuable. We will be reporting on the link between OCT and rod and cone abnormalities in a future paper.

Conclusion

In summary, we showed that, in early AMD, the presence of abnormalities in the fundus photograph and in FAF correspond closely to scotopic and photopic changes in visual function. As far as dynamic measures are concerned, parameter S2, exclusively mediated by rods, is the best predictor of both structural measures of abnormality. It is important to note, however, that α is also grossly abnormal in all cases. As described in our previous paper,[40] α offers a unique measure of the dynamics of cone-based sensitivity recovery.

CS is a static measure, also mediated by cones, and it correlates strongly with FAF but less well with fundus photograph grade. It is clear that dynamic and static measures complement each other; therefore, combining S2 and α from DA measurements with CS seems to be an optimal approach when evaluating functional loss in early/intermediate AMD.

Any future management strategy for dry AMD must be focused on minimizing progress at the earliest possible stage of the disease. Therapies can be expected to be most effective at these early stages, so accurately identifying the high-risk patients will be crucial. Identifying these individuals will be most precise when morphologic changes are combined with the functional changes described here.

Acknowledgments

The authors thank all reviewers for insightful comments.

Supported by the Manchester Biomedical Research Centre and the Greater Manchester Comprehensive Local Research Network (NRAP, TMA), Newtricious R&D B.V. (HJT, ER-D, TMA, NRAP), and the National Eye Research Centre (ER-D).

Disclosure: **E. Rodrigo-Diaz**, Newtricious (F), National Eye Research Centre, UK (F); **H.J. Tahir**, Newtricious (F); **J.M. Kelly**, None; **N.R.A. Parry**, None; **T. Aslam**, None; **I.J. Murray**, None

References

1. Acton JH, Smith RT, Hood DC, Greenstein VC. Relationship between retinal layer thickness and the visual field in early age-related macular degeneration. *Invest Ophthalmol Vis Sci*. 2012;53:7618–7624.
2. Bunce C, Xing W, Wormald R. Causes of blind and partial sight certifications in England and Wales: April 2007-March 2008. *Eye (Lond)*. 2010;24:1692–1699.
3. Klein R, Klein BE, Linton KL. Prevalence of age-related maculopathy: the Beaver Dam Eye Study. *Ophthalmology*. 1992;99:933–943.
4. Friedman DS, O'Colmain BJ, Munoz B, et al. Prevalence of age-related macular degeneration in the United States. *Arch Ophthalmol*. 2004;122:564–572.
5. Penfold PL, Provis JM. *Macular Degeneration*. Berlin: Springer; 2005.
6. Seddon JM, Cote J, Rosner B. Progression of age-related macular degeneration: association with dietary fat, transunsaturated fat, nuts, and fish intake. *Arch Ophthalmol*. 2003;121:1728–1737.
7. Chakravarthy U, Wong TY, Fletcher A, et al. Clinical risk factors for age-related macular degeneration: a systematic review and meta-analysis. *BMC Ophthalmol*. 2010;10:31.
8. Chakravarthy U, Augood C, Bentham GC, et al. Cigarette smoking and age-related macular degeneration in the EUREYE Study. *Ophthalmology*. 2007;114:1157–1163.
9. Seddon JM, Reynolds R, Yu Y, Daly MJ, Rosner B. Risk models for progression to advanced age-related macular degeneration using demographic, environmental, genetic, and ocular factors. *Ophthalmology*. 2011;118:2203–2211.
10. Popescu ML, Boisjoly H, Schmaltz H, et al. Explaining the relationship between three eye diseases and depressive symptoms in older adults. *Invest Ophthalmol Vis Sci*. 2012; 53:2308–2313.
11. Lamoureux EL, Mitchell P, Rees G, et al. Impact of early and late age-related macular degeneration on vision-specific functioning. *Br J Ophthalmol*. 2011;95:666–670.
12. Bird AC, Bressler NM, Bressler SB, et al; The International ARM Epidemiological Study Group. An international classification and grading system for age-related maculopathy and age-related macular degeneration. *Surv Ophthalmol*. 1995;39: 367–374.
13. Ferris FL, Wilkinson CP, Bird A, et al. Clinical classification of age-related macular degeneration. *Ophthalmology*. 2013;120: 844–851.
14. Ferris FL, Davis MD, Clemons TE, et al. A simplified severity scale for age-related macular degeneration: AREDS Report No. 18. *Arch Ophthalmol*. 2005;123:1570–1574.

15. Bindewald A, Bird AC, Dandekar SS, et al. Classification of fundus autofluorescence patterns in early age-related macular disease. *Invest Ophthalmol Vis Sci*. 2005;46:3309–3314.
16. Landa G, Rosen RB, Pilavas J, Garcia PM. Drusen characteristics revealed by spectral-domain optical coherence tomography and their corresponding fundus autofluorescence appearance in dry age-related macular degeneration. *Ophthalmic Res*. 2012;47:81–86.
17. Wu Z, Luu CD, Ayton LN, et al. Optical coherence tomography-defined changes preceding the development of drusen-associated atrophy in age-related macular degeneration. *Ophthalmology*. 2014;121:2415–2422.
18. Ooto S, Suzuki M, Vongkulsiri S, Sato T, Spaide RF. Multimodal visual function testing in eyes with nonexudative age-related macular degeneration. *Retina*. 2015;35:1726–1734.
19. Fraser RG, Tan R, Ayton LN, Caruso E, Guymer RH, Luu CD. Assessment of retinotopic rod photoreceptor function using a dark-adapted chromatic perimeter in intermediate age-related macular degenerationdark-adapted chromatic perimetry in intermediate AMD. *Invest Ophthalmol Vis Sci*. 2016;57:5436–5442.
20. Delori FC, Dorey CK, Staurenghi G, Arend O, Goger DG, Weiter JJ. In vivo fluorescence of the ocular fundus exhibits retinal pigment epithelium lipofuscin characteristics. *Invest Ophthalmol Vis Sci*. 1995;36:718–729.
21. Weiter JJ, Delori FC, Wing GL, Fitch KA. Retinal pigment epithelial lipofuscin and melanin and choroidal melanin in human eyes. *Invest Ophthalmol Vis Sci*. 1986;27:145–152.
22. Greenberg JP, Duncker T, Woods RL, Smith RT, Sparrow JR, Delori FC. Quantitative fundus autofluorescence in healthy eyes. *Invest Ophthalmol Vis Sci*. 2013;54:5684–5693.
23. Berendschot TT, van Norren D. Objective determination of the macular pigment optical density using fundus reflectance spectroscopy. *Arch Biochem Biophys*. 2004;430:149–155.
24. Han M, Giese G, Schmitz-Valckenberg S, et al. Age-related structural abnormalities in the human retina-choroid complex revealed by two-photon excited autofluorescence imaging. *J Biomed Opt*. 2007;12:024012.
25. Holz FG, Bindewald-Wittich A, Fleckenstein M, et al. Progression of geographic atrophy and impact of fundus autofluorescence patterns in age-related macular degeneration. *Am J Ophthalmol*. 2007;143:463–472.
26. Delori FC, Fleckner MR, Goger DG, Weiter JJ, Dorey CK. Autofluorescence distribution associated with drusen in age-related macular degeneration. *Invest Ophthalmol Vis Sci*. 2000;41:496–504.
27. Kleiner RC, Enger C, Alexander MF, Fine SL. Contrast sensitivity in age-related macular degeneration. *Arch Ophthalmol*. 1988;106:55–57.
28. Patel PJ, Chen FK, Da Cruz L, Rubin GS, Tufail A; the ABC Trial Group. Contrast sensitivity outcomes in the ABC Trial: a randomized trial of bevacizumab for neovascular age-related macular degeneration. *Invest Ophthalmol Vis Sci*. 2011;52:3089–3093.
29. Faria BM, Duman F, Zheng CX, et al. Evaluating contrast sensitivity in age-related macular degeneration using a novel computer-based test, the Spaeth/Richman contrast sensitivity test. *Retina*. 2015;35:1465–1473.
30. Owsley C, Huisingh C, Clark ME, Jackson GR, McGwin G Jr. Comparison of visual function in older eyes in the earliest stages of age-related macular degeneration to those in normal macular health. *Curr Eye Res*. 2016;41:266–272.
31. Midena E, Degli Angeli C, Blarzino MC, Valenti M, Segato T. Macular function impairment in eyes with early age-related macular degeneration. *Invest Ophthalmol Vis Sci*. 1997;38:469–477.
32. Feigl B, Brown B, Lovie-Kitchin J, Swann P. Cone-mediated multifocal electroretinogram in early age-related maculopathy and its relationships with subjective macular function tests. *Curr Eye Res*. 2004;29:327–336.
33. Steinmetz RL, Haimovici R, Jubb C, Fitzke FW, Bird AC. Symptomatic abnormalities of dark adaptation in patients with age-related Bruch's membrane change. *Br J Ophthalmol*. 1993;77:549–554.
34. Curcio CA, Owsley C, Jackson GR. Spare the rods, save the cones in aging and age-related maculopathy. *Invest Ophthalmol Vis Sci*. 2000;41:2015–2018.
35. Curcio CA, Sloan KR, Kalina RE, Hendrickson AE. Human photoreceptor topography. *J Comp Neurol*. 1990;292:497–523.
36. Jackson GR, Owsley C, Curcio CA. Photoreceptor degeneration and dysfunction in aging and age-related maculopathy. *Ageing Res Rev*. 2002;1:381–396.
37. Owsley C, Jackson GR, Cideciyan AV, et al. Psychophysical evidence for rod vulnerability in age-related macular degeneration. *Invest Ophthalmol Vis Sci*. 2000;41:267–273.
38. Dimitrov PN, Guymer RH, Zele AJ, Anderson AJ, Vingrys AJ. Measuring rod and cone dynamics in age-related maculopathy. *Invest Ophthalmol Vis Sci*. 2008;49:55–65.
39. Rodrigo-Diaz E, Tahir HJ, Parry NRA, et al. A novel technique for measuring dark adaptation using a dual stimulus method: effects of aging and AMD on dark adaptation. *Acta Ophthalmol*. 2014;92:T010.
40. Tahir HJ, Rodrigo-Diaz E, Parry NRA, et al. Slowed dark adaptation in early AMD: dual stimulus reveals scotopic and photopic abnormalities. *Invest Ophthalmol Vis Sci*. 2018;59:AMD202–AMD210.
41. Lamb TD. The involvement of rod photoreceptors in dark adaptation. *Vision Res*. 1981;21:1773–1782.
42. Lamb TD, Pugh EN Jr. Phototransduction, dark adaptation, and rhodopsin regeneration the proctor lecture. *Invest Ophthalmol Vis Sci*. 2006;47:5137–5152.
43. Pugh EN. Rushton's paradox: rod dark adaptation after flash photolysis. *J Physiol*. 1975;248:413–431.
44. Owsley C, McGwin G Jr, Clark ME, et al. Delayed rod-mediated dark adaptation is a functional biomarker for incident early age-related macular degeneration. *Ophthalmology*. 2016;123:344–351.
45. Dimitrov PN, Robman LD, Varsamidis M, et al. Visual function tests as potential biomarkers in age-related macular degeneration. *Invest Ophthalmol Vis Sci*. 2011;52:9457–9469.
46. Dimitrov PN, Robman LD, Varsamidis M, et al. Relationship between clinical macular changes and retinal function in age-related macular degeneration. *Invest Ophthalmol Vis Sci*. 2012;53:5213–5220.
47. Luu CD, Dimitrov PN, Wu Z, et al. Static and flicker perimetry in age-related macular degeneration. *Invest Ophthalmol Vis Sci*. 2013;54:3560–3568.
48. Sevilla MB, McGwin G Jr, Lad EM, et al. Relating retinal morphology and function in aging and early to intermediate age-related macular degeneration subjects. *Am J Ophthalmol*. 2016;165:65–77.
49. Lamb TD, Pugh EN Jr. Dark adaptation and the retinoid cycle of vision. *Prog Retin Eye Res*. 2004;23:307–380.
50. Jackson GR, Clark ME, Scott IU, Walter LE, Quillen DA, Brigell MG. Twelve-month natural history of dark adaptation in patients with AMD. *Optom Vis Sci*. 2014;91:925–931.
51. Murray I, Carden D, Kelly JM. New rapid digital dark adaptometer that shows high sensitivity and specificity for early AMD. *Invest Ophthalmol Vis Sci*. 2016;57:3705–3705.
52. Age-Related Eye Disease Study Research Group. The Age-Related Eye Disease Study system for classifying age-related macular degeneration from stereoscopic color fundus photographs: the Age-Related Eye Disease Study Report Number 6. *Am J Ophthalmol*. 2001;132:668–681.

Investigative Ophthalmology & Visual Science

53. Elliott DB, Sanderson K, Conkey A. The reliability of the Pelli-Robson contrast sensitivity chart. *Ophthalmic Physiol Opt*. 1990;10:21–24.
54. Tahir HJ, Rodrigo-Diaz E, Parry NRA, Kelly JMF, Carden D, Murray IJ. Slowed dark adaptation in older eyes; effect of location. *Exp Eye Res*. 2017;155:47–53.
55. Patryas L, Parry NR, Carden D, et al. Assessment of age changes and repeatability for computer-based rod dark adaptation. *Graefes Arch Clin Exp Ophthalmol*. 2013;251:1821–1827.
56. Tahir HJ, Cerio E, Parry NRA, et al. Novel dual arc stimulus aids sensitive detection of early AMD. *Invest Ophthalmol Vis Sci*. 2015;56:2617–2617.
57. Tahir H, Murray I, Carden D, Parry N. Sensitivity recovery following a bleach: a dual "smiley" arc stimulus technique for studying abnormal dark adaptation. *Invest Ophthalmol Vis Sci*. 2013;54:2767–2767.
58. McGwin G Jr, Jackson GR, Owsley C. Using nonlinear regression to estimate parameters of dark adaptation. *Behav Res Methods Instrum Comput*. 1999;31:712–717.
59. Landa G, Su E, Garcia PM, Seiple WH, Rosen RB. Inner segment-outer segment junctional layer integrity and corresponding retinal sensitivity in dry and wet forms of age-related macular degeneration. *Retina*. 2011;31:364–370.
60. Jackson GR, Owsley C, McGwin G Jr. Aging and dark adaptation. *Vision Res*. 1999;39:3975–3982.
61. Curcio CA, Johnson M, Rudolf M, Huang JD. The oil spill in ageing Bruch membrane. *Br J Ophthalmol*. 2011;95:1638–1645.
62. Owsley C, McGwin G Jr, Jackson GR, Kallies K, Clark M. Cone- and rod-mediated dark adaptation impairment in age-related maculopathy. *Ophthalmology*. 2007;114:1728–1735.
63. Scilley K, Jackson GR, Cideciyan AV, Maguire MG, Jacobson SG, Owsley C. Early age-related maculopathy and self-reported visual difficulty in daily life. *Ophthalmology*. 2002;109:1235–1242.
64. Midena E, Vujosevic S, Convento E, Manfre A, Cavarzeran F, Pilotto E. Microperimetry and fundus autofluorescence in patients with early age-related macular degeneration. *Br J Ophthalmol*. 2007;91:1499–1503.
65. Scholl HP, Bellmann C, Dandekar SS, Bird AC, Fitzke FW. Photopic and scotopic fine matrix mapping of retinal areas of increased fundus autofluorescence in patients with age-related maculopathy. *Invest Ophthalmol Vis Sci*. 2004;45:574–583.
66. Gliem M, Muller PL, Finger RP, McGuinness MB, Holz FG, Charbel Issa P. Quantitative fundus autofluorescence in early and intermediate age-related macular degeneration. *JAMA Ophthalmol*. 2016;134:817–824.

Investigative Ophthalmology & Visual Science